Nuclear Instruments and Methods in Physics Research B 310 (2013) 1–5

Contents lists available at SciVerse ScienceDirect

Nuclear Instruments and Methods in Physics Research B

journal homepage: www.elsevier.com/locate/nimb

Ion irradiation induced order-to-disorder transformation in δ-phase $Lu_4Hf_3O_{12}$

J. Wen [a], C. Gao [a], Y.H. Li [a,*], Y.Q. Wang [b], L.M. Zhang [a], B.T. Hu [a], L.J. Chen [a], X. Su [a]

[a] School of Nuclear Science and Technology, Lanzhou University, Lanzhou 730000, China
[b] Materials Science and Technology Division, Los Alamos National Laboratory, Los Alamos, NM 87545, USA

ARTICLE INFO

Article history:
Received 12 December 2012
Received in revised form 12 April 2013
Available online 9 May 2013

Keywords:
Ion irradiation
δ-$Lu_4Hf_3O_{12}$
Order-to-disorder transformation

ABSTRACT

In this study, polycrystalline δ-phase $Lu_4Hf_3O_{12}$ was irradiated with 6 MeV Xe^{26+} ions to fluences ranging from 2×10^{13} to 1×10^{15} ions/cm^2. Ion irradiation-induced microstructural evolution was examined by using grazing incidence X-ray diffraction (GIXRD). A complete phase transformation from ordered rhombohedral to disordered fluorite (O–D) was observed by a fluence of 1×10^{15} ions/cm^2, equivalent to a peak ballistic damage dose of ~3.49 displacements per atom (dpa). To research the different irradiation effect between light ion and heavy ion on δ-$Lu_4Hf_3O_{12}$, 400 keV Ne^{2+} ions were implanted to ion fluences ranging from 1×10^{14} to 1×10^{15} ions/cm^2. A complete O–D crystal structure transformation was observed by a fluence of 5×10^{14} ions/cm^2 (~0.22 dpa). This threshold dose was found to be observably lower than the threshold dose to produce order-to-disorder transformation using Xe^{26+} ions on δ-$Lu_4Hf_3O_{12}$. This suggests that heavy ions are less efficient than light ions in producing the retained defects that are responsible for the O–D transformation. The theoretical calculations show that the O–D transformation of δ-phase was attributed to the anion oxygen Frenkel pair defect. The ion irradiation-induced transformation of δ-phase $Lu_4Hf_3O_{12}$ into disordered fluorite structure observed here is also discussed in relation to the temperature–composition (T–C) phase diagrams for the compound.

© 2013 Elsevier B.V. All rights reserved.

1. Introduction

During the last decade, the search for radiation-tolerant materials that can be used as host materials for minor actinides or high-level radioactive waste has been the focus of many studies [1–7]. Recent research has focused significant interest on an important class of materials that possess structures related to the fluorite (CaF_2) crystal structure. The oxide fluorite, with stoichiometry MO_2 (M is a metal cation, O an oxygen anion), is a face-centered cubic structure belonging to space group $Fm\bar{3}m$ (No. 225 in the International Tables for Crystallography). Our interest here is in oxygen-deficient fluorite structural derivative (MO_{2-x}) compounds. In oxygen-deficient compounds, the valences of metal cations have several valence states (A^{1+}, A^{2+}, or A^{3+}) to achieve a charge balance. Certain oxygen-deficient fluorite structural derivatives include: (1) bixbyite, an M_2O_3 sesquioxide [8,9]; (2) pyrochlore, an M_4O_7 compound (more specifically $A^{3+}{}_2B^{4+}{}_2O_7$) [10,11]; (3) δ-phase, an M_7O_{12} compound (more specifically $A^{3+}{}_4B^{4+}{}_3O_{12}$) which possess rhombohedral symmetry and belongs to space group $R\bar{3}$ [1,12]. Such materials exhibit radiation tolerant properties [8–12].

In previous studies, no "4:3:12" δ-phase compounds have exhibited irradiation-induced amorphization. For example, $Sc_4Zr_3O_{12}$ cannot be amorphized even at very high radiation dose (~70 dpa) [13]. However, δ-phase compounds do undergo an order-to-disorder (O–D) transformation, from ordered δ-phase to disordered fluorite (F) phase, when exposed to ion irradiation. Interestingly, the threshold doses to produce an O–D transformation using light ions in $A_4Zr_3O_{12}$ compounds were found to be significantly lower than that using heavy ions [12–14]. The particular compound of interest here is δ-$Lu_4Hf_3O_{12}$ that nobody has previously researched. This study considers the phase transformation and the irradiation effects of the light and heavy ions on this compound. The effect of irradiation-induced cation antisite and anion oxygen Frenkel-pair defects on the O–D transformation is also discussed.

2. Experimental procedure

Polycrystalline $Lu_4Hf_3O_{12}$ samples were synthesized from HfO_2 (Aldrich Chemical company, 99.99% purity) and Lu_2O_3 (Alfa Aesar, 99.99% purity) powders, by conventional ceramic processing procedures. Sample wafers were then cut and polished to a mirror finish using W0.25 Diamond suspension. X-ray diffraction measurements revealed that these samples possess a rhombohedral symmetry, δ-phase.

The experimental work was carried out at the 320 kV platform for multi-discipline research with highly charged ions at the Institute of Modern Physics, CAS. Six mega electron volt Xe^{26+} ion irra-

* Corresponding author. Tel.: +86 13893622587.
E-mail address: liyuhong@lzu.edu.cn (Y.H. Li).

0168-583X/$ - see front matter © 2013 Elsevier B.V. All rights reserved.
http://dx.doi.org/10.1016/j.nimb.2013.04.055

diation was performed at normal incidence relative to the sample surface, to ion fluences ranging from 2×10^{13} to 1×10^{15} ions/cm^2. The average ion flux was maintained at $\sim1\times10^{11}$ ions/cm^2 s during implantation. The projected range of 6 MeV Xe^{26+} ions in δ-$Lu_4Hf_3O_{12}$ was estimated by using the Monte Carlo code SRIM [15]. The projected range, R_p, was estimated to be 0.99 μm (with a target density ρ = 10.05 g/cm^3 of $Lu_4Hf_3O_{12}$), with a longitudinal straggling, ΔR_p, of 0.31 μm. In these SRIM calculations, we arbitrarily assume the threshold displacement energies of Lu, Hf and O are all 40 eV (because we currently do not have theoretical or experimental estimates for these values) [12,16]. Fig. 1 shows the results of SRIM simulations of $Lu_4Hf_3O_{12}$ by 6 MeV Xe^{26+} and 400 keV Ne^{2+} ion irradiation, respectively. Obviously, electronic stopping plays a significant role in the total stopping energy for both Xe and Ne ions. Table 1 shows Monte Carlo simulation estimates of various displacement damage parameters for 6 MeV Xe and 400 keV Ne ions irradiation in $Lu_4Hf_3O_{12}$.

Grazing Incidence X-ray Diffraction (GIXRD) was used to analyze the crystal structure of the pristine and ion irradiated samples using a Rigaku D/Max-2400 X-ray Diffractometer, Cu-K_α radiation, $\theta-2\theta$ geometry, and X-ray angle of incidence of γ = 5°. The $\theta-2\theta$ scans were performed using a step size of 0.02° and a dwell time of one second. The scan range was 15–65°. The depth of the X-ray in $Lu_4Hf_3O_{12}$ at γ = 5° is 0.56 μm, which corresponds to the maximum depth where electronic energy loss starts to decreases sharply.

To contrast light ion and heavy ion irradiation effects in $Lu_4Hf_3O_{12}$, we carried out another ion irradiation experiment using 400 keV Ne^{2+} ions. Ion irradiation was performed in the Ion Beam Material Laboratory at Los Alamos National Laboratory using a 200-kV Danfysik High Current Research Ion Implanter. The 400 keV Ne^{2+} ions were implanted at normal incidence of fluences ranging from 1×10^{14} to 1×10^{15} ions/cm^2, using an ion flux of $\sim1\times10^{12}$ ions/cm^2 s. GIXRD measurements were made using a Bruker AXS D8 advanced X-ray diffractometer, Cu-K_α radiation, $\theta-2\theta$ geometry, and the X-ray angle of incidence of γ = 3°. The depth of the X-ray in $Lu_4Hf_3O_{12}$ at γ = 3° is 0.31 μm, which also corresponds to the maximum depth where electronic energy loss starts to decreases sharply.

3. Results

Fig. 2 shows GIXRD patterns obtained from pristine $Lu_4Hf_3O_{12}$ and $Lu_4Hf_3O_{12}$ irradiated with 6 MeV Xe^{26+} ions to fluences of 2×10^{13} to 1×10^{15} ions/cm^2. These fluences correspond to peak displacement damage doses of ~0.07–3.49 dpa. The X-ray incidence angle for these measurements was chosen as γ = 5°, based on the critical angle calculations from Refs. [17,18]. Under these conditions, X-rays are scattered from the near surface of the sample [18,19]. This is much smaller than the 6 MeV Xe^{26+} ion range (~1.0 μm). Therefore, the GIXRD measurements sample only the irradiated section, in the vicinity of the sample surface. The peaks labeled "δ" of the pristine sample in Fig. 2 represent the rhombohedral structure, δ-phase. These "superlattice" reflections diminished by a fluence of 2×10^{13} ions/cm^2 and completely disappeared at the highest fluence of 1×10^{15} ions/cm^2. It was observed clearly that δ{1 1 0} and δ{0 1 2} peaks disappeared gradually with increasing Xe ion fluence, shown in the inserted diagram of Fig. 2. At the same time, the four most prominent diffraction peaks, which are associated with the "parent" fluorite structure (labeled "F" in the GIXRD pattern in Fig. 1) are more or less unaffected by irradiation. These observations imply that Xe^{26+} ion irradiation of $Lu_4Hf_3O_{12}$ induces an O–D transformation, from an ordered δ-phase structure to a disordered cubic fluorite structure.

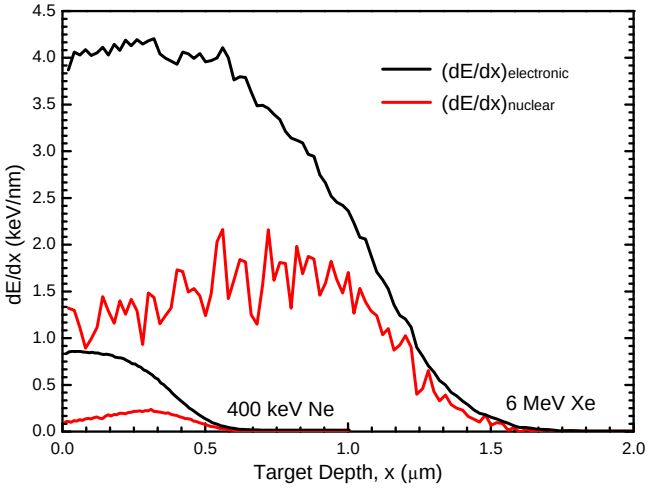

Fig. 1. Monte Carlo simulation estimates of electronic vs. nuclear energy loss for 6 MeV Xe ions and 400 keV Ne ions as functions of penetration depth for $Lu_4Hf_3O_{12}$.

Table 1
SRIM 2008 calculations for 6 MeV Xe and 400 keV Ne ion irradiation in $Lu_4Hf_3O_{12}$ at a fluence of 1×10^{15} ions/cm^2.

Ions	6 MeV Xe	400 keV Ne
Sample depth at peak concentration (μm)	1.20	0.36
Ion peak concentration (at.%)	3.92	2.95
Sample depth at peak dpa (μm)	0.88	0.31
Peak dpa	3.49	0.44

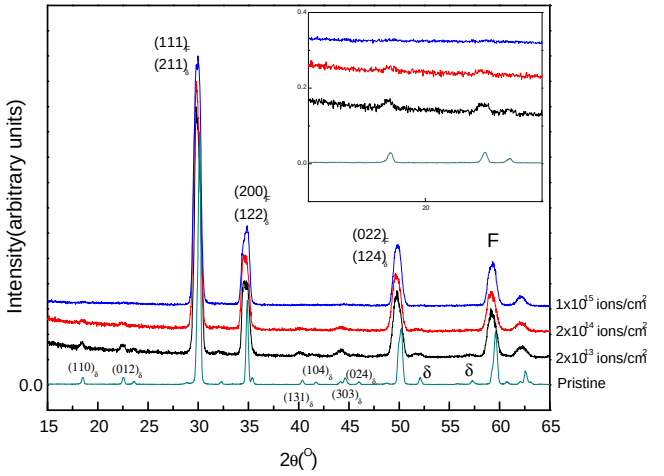

Fig. 2. GIXRD patterns obtained from pristine and irradiated $Lu_4Hf_3O_{12}$ samples with 6-MeV Xe^{26+} ions to dose of 2×10^{13}–1×10^{15} ions/cm^2 at X-ray incidence angle of 5°. Peaks labeled "δ" are due to the superlattice reflections associated with the ordered δ-phase, while the peaks labeled "F" are the parent fluorite structure. The inserted diagram was the zoomed on main δ-phase peaks, {1 1 0} and {0 1 2}.

Fig. 3 shows GIXRD patterns obtained from $Lu_4Hf_3O_{12}$ before and after 400 keV Ne^{2+} ion irradiation. The absence of the δ-phase reflections with increasing dose reveals that $Lu_4Hf_3O_{12}$ undergoes an O–D transformation, from an ordered δ-phase structure to a disordered fluorite structure. An complete O–D crystal structure transformation was observed by a fluence of 5×10^{14} ions/cm^2 (~0.22 dpa).

4. Discussion

Our 400 keV Ne^{2+} ion irradiation results show the same irradiation-resistant trend as that from 6 MeV Xe^{26+} ion irradiation: δ-$Lu_4Hf_3O_{12}$ does undergo a phase transformation from an ordered δ-phase rhombohedral structure to a disordered fluorite

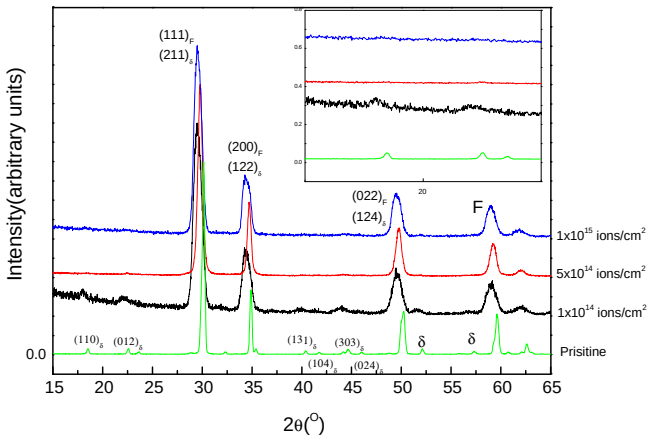

Fig. 3. GIXRD patterns obtained from pristine and irradiated $Lu_4Hf_3O_{12}$ samples with 400-keV Ne^{2+} ions to dose of 1×10^{14}–1×10^{15} ions/cm^2 at X-ray incidence angle of 3°. Peaks labeled "δ" are due to the superlattice reflections associated with the ordered δ-phase, while the peaks labeled "F" are the parent fluorite structure. The inserted diagram was the zoomed on main δ-phase peaks, {1 1 0} and {0 1 2}.

cubic structure with the disappearance of "superlattice" reflections following different ion irradiations.

In this section, to understand the change in O–D transformation, we will discuss in terms of a new layered atom stacking model for the compound [20]. Firstly, we should consider the cubic fluorite structure MO_2. Along the $\bar{3}$ direction, there is a layer atom stacking motif that repeats in the following sequence: MOVO. It is necessary to fully describe the fluorite structure by 12 layers, MOVOMOVO-MOVO, where all atom layers represent fully-dense triangular nets. All layers are atomically pure: M is a layer consisting only of cations and O is a pure layer of oxygen anions, V represents a completely vacant layer. The stacking sequence is shown in Fig. 4(a) for a general MO_2 fluorite.

Now we consider the layer stacking sequence in δ-$Lu_4Hf_3O_{12}$ according to the previous discussion. For convenience, we describe our rhombohedral, δ-phase structure using a hexagonal unit cell. There are 12 layers (three M layers and six O layers) per hexagonal unit cell along the *c* axis. The stacking sequence of the δ-$Lu_4Hf_3O_{12}$ is the same as the MOVO sequence found in MO_2 fluorite. But there have only one different that the atoms in M and O layers shown in Fig. 4(b) are rumpled out-of-plane along $\bar{3}$ in δ-$Lu_4Hf_3O_{12}$ (atom position deviations from ideality are less than 4%) [20]. Fig. 5 illustrates the atomic arrangements in the M and O layers in δ-$Lu_4Hf_3O_{12}$. The M layer consists of metal cations is based on triangular atom nets, where Lu and Hf atoms are randomly arranged (Fig. 5(a)). The O layer consists of oxygen anions, also in a triangular atom nets, but contains ordered empty sites within each layer (Fig. 5(b)). The O layer tiling pattern is analogous to a $3^4.6$ Archimedean tiling. Each O layer consists of 6/7 dense (partially-dense), while each M layer is 7/7 dense (fully-dense).

Numerous studies of pyrochlore compounds have been performed [16,21,22]. Although different pyrochlores showed great disparity of structure transformation under ion irradiation, e.g. most zirconate pyrochlores experience an obvious order-to-disorder transformation and are more resistant to the irradiation damage,

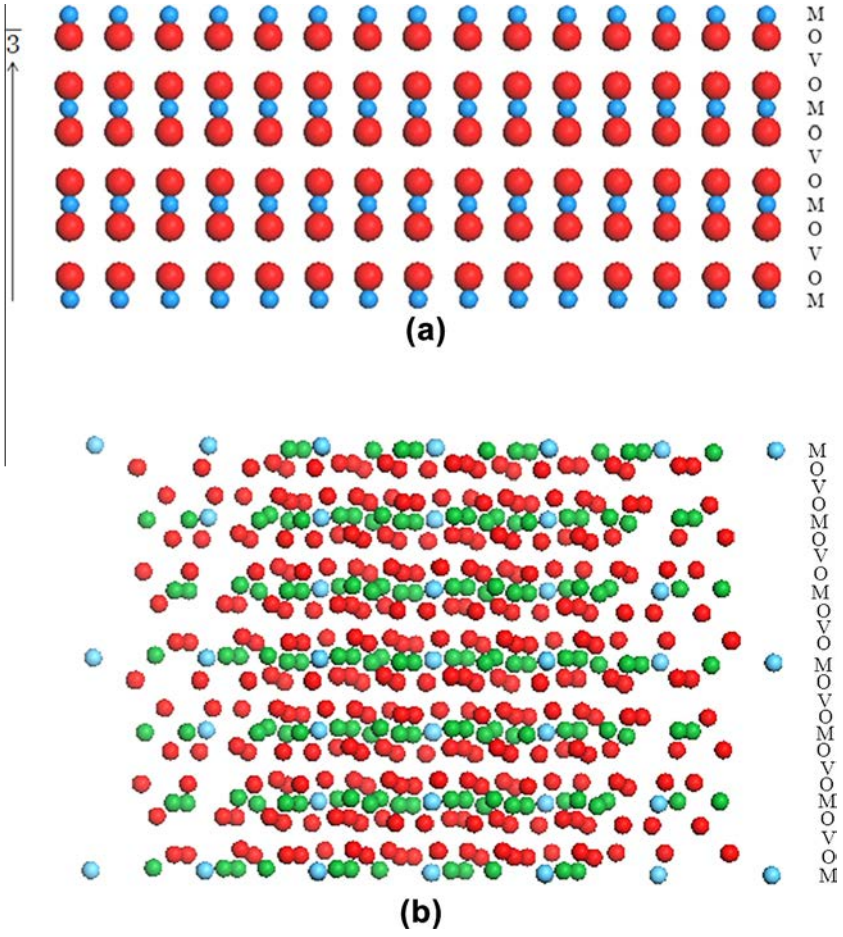

Fig. 4. (a) Schematic diagram illustrates the layer stacking sequence along the $\bar{3}$ axis in a cubic fluorite compound. M and O represent pure metal cation and pure oxygen anion layers, respectively. The stacking sequence is MOVOMOVOMOVO, where V represents an empty layer. (b) Along the $\bar{3}$ direction, the layer stacking sequence of rhombohedral δ-$Lu_4Hf_3O_{12}$ is identical to the sequence shown here, except that the atoms are slightly out-of-plane about 2–3% (contain four unit cell).

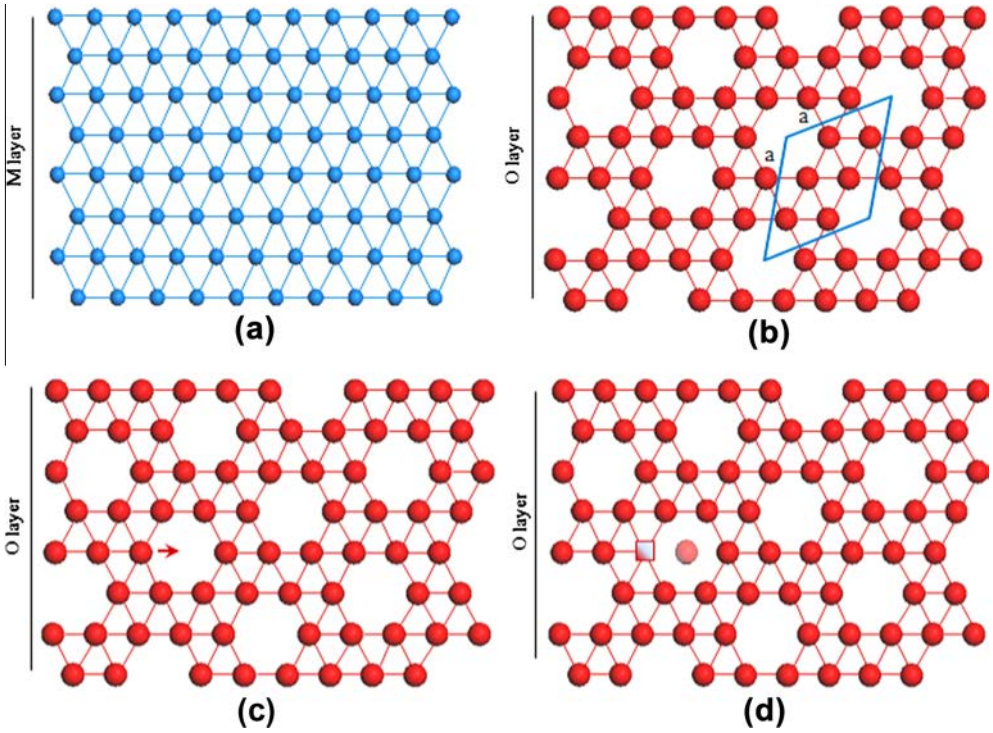

Fig. 5. Schematic diagram showing the stacking of the layers along the *c*-axis for the hexagonal description of δ-phase $Lu_4Hf_3O_{12}$, and illustrates a simple Frenkel diffusion mechanism for this compound. (a) cation (M) layer atom arrangement based on triangular atom nets with full dense. Lu and Hf atoms are randomly arranged. Each M site is occupied statistically by 4 of 7 Lu and 3 of 7 Hf atoms. (b) Oxygen atoms are arranged in a $3^4{\cdot}6$ Archimedean tiling pattern. The base of the δ-phase hexagonal unite cell is described in the drawing (edge lengths equal to lattice parameter, (a). The atoms in real δ-$Lu_4Hf_3O_{12}$ relax slightly away from the perfect triangular atom net in (a) and the $3^4{\cdot}6$ Archimedean tiling pattern in (b). (c) An oxygen layer, with the jump direction for an atom near the vacancy. (d) The atom arrangement following the jump of the atom in (c) into the vacancy in the tiling pattern. The interstitial O atom is low-light in red. The vacancy left is shown as a red-shaded square. Diagrams (c) and (d) represent radiation-induced anion disorder. (For interpretation of the references to color in this figure legend, the reader is referred to the web version of this article.)

while titanate pyrochlores undergo significant volume swelling before readily succumbing to amorphization under ion irradiation, both zirconate and titanate pyrochlores experience lattice disorder under ion irradiation. Detailed theoretical analyses demonstrated that cation antisite-pair defects are the main defects that cause the lattice disorder of the pyrochlores under ion irradiation. Jie et al. pointed out that cation antisite-pair defects formed directly during cascades, while anion-disorder was promoted by cation antisite (oxygen atoms are randomly distributed in O lattice). In order to predict the effect of cation antisite-pair defect in phase transformation for δ-$Lu_4Hf_3O_{12}$, we calculated the intensity ratio of {0 1 2} over {2 1 1} as a function of cation disordering, {0 1 2} is the ordered rhombohedral δ-phase superlattice reflection; while {2 1 1} is fundamental fluorite reflection, as shown in Fig. 6. The result shows that the intensity ratio of I{0 1 2}/I{2 1 1} is almost a constant, independently on the amount of Lu and Hf cation antisite pairs, which indicates that the order-to-disorder transformation in δ-$Lu_4Hf_3O_{12}$ is not due to the cation antisite defects. Certainly, we can come to a conclusion that the order-to-disorder phase transformation in δ-$Lu_4Hf_3O_{12}$ must be caused by anion oxygen Frenkel defect.

To summarize, the weak superlattice reflections observed in the GIXRD is apparently due to the ordered O atoms arrangement. If the ordered anion rearranged upon ion irradiation, the structure transformation of δ-$Lu_4Hf_3O_{12}$ would happen from order to disorder (rhombohedral to cubic). This is precisely what is observed in these experiments. The irradiation-induced O–D transformation induced by O Frenkel pair formation is shown in Fig. 5(c). O atoms on proper sites would spontaneously displace into the vacant O sites during irradiation, until the vacancies in the O layers are randomly distributed (Fig. 5(d)). In time, the compound transformed from ordered rhombohedral structure to disordered fluorite cubic structure.

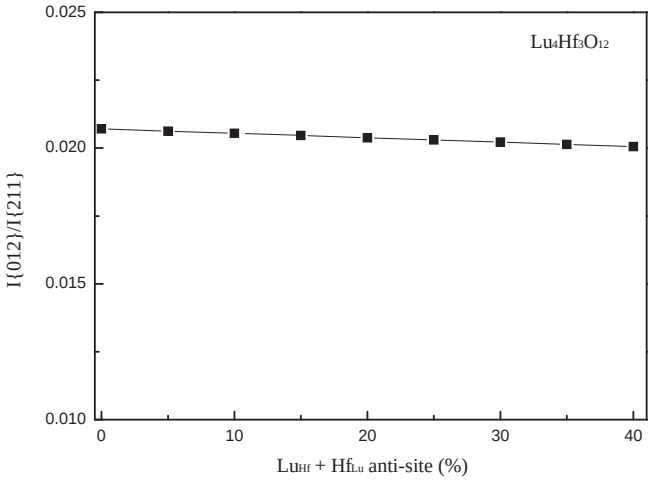

Fig. 6. Relationship of I{0 1 2}/I{2 1 1} of $Lu_4Hf_3O_{12}$ with the amount of Lu and Hf antisite pairs.

Moreover, our group has also calculated the role of the cation/anion defects on the structural transformation in δ-phase compounds A_6BO_{12} (A = Gd, Ho, Y; B = U, W), which possess the same structure with compounds $A_4B_3O_{12}$. The theoretical calculations (not shown here) indicate that the anion oxygen Frenkel defects play a significant role in the irradiation-induced O–D transformation process of δ-phase, though anion-disorder is promoted by cation antisite [23].

Another interesting phenomenon showed here is that although both heavy (Xe) and light (Ne) ion irradiations can induce an O–D

transformation from an ordered δ-phase rhombohedral to a disordered fluorite cubic structure in δ-$Lu_4Hf_3O_{12}$, the O–D transformation threshold doses were observably different between heavy and light ions. Under 6 MeV Xe^{26+} ion irradiation, the O–D transformation for δ-$Lu_4Hf_3O_{12}$ occurred at 1×10^{15} ions/cm^2 (~3.49 dpa). However, under 400 keV Ne^{2+} ion irradiation, the O–D transformation occurred at 5×10^{14} ions/cm^2 (~0.22 dpa). This is so-called "ion spectrum effect" [24–26]. The different threshold doses observed between heavy and light ions are likely related to the Frenkel defects recombination and survival efficiency. This spectrum effect was observed previously on the same structure compound, δ-$Sc_4Zr_3O_{12}$ [14]. Now, here a similar result is firstly discovered on δ-$Lu_4Hf_3O_{12}$. To best understand this effect, morphological characteristics of ion irradiation damage were estimated using the Monte Carlo code SRIM [15]. The heavy Xe ion produces ~24,500 vacancy–interstitial Frenkel pairs per ion near a range of ~1.0 μm, while the light Ne ion produces ~1400 vacancy–interstitial Frenkel pairs per ion near a range of ~0.31 μm. It implies that the displacement cascades produced by 6 MeV Xe ions are more dense compared to displacement cascades produced by 400 keV Ne ions. In other words, Frenkel point defects produced by Ne ions have a lower annihilating probability, such as interstitial/vacancy recombination, than that produced by Xe ions. As a result, more defects produced by Ne ions could survive than Xe ions in the δ-$Lu_4Hf_3O_{12}$ compounds. Consequently, heavy Xe ions need higher irradiation fluences to induce O–D phase transformation in δ-$Lu_4Hf_3O_{12}$ than the light Ne ions.

Another reasonable mechanism for O–D transformation different threshold dose between heavy and light ions is the energy transfer kinetic factor. On the basis of collision theory between two rigid balls, the energy transfer kinetic factor can be expressed by $\wedge = 4m_1m_2/(m_1+m_2)^2$, where m_1 and m_2 are the atomic masses of two balls. According to this formula, the capability of oxygen displacement would be due to the atomic masses of incident ion and oxygen. For Ne and O, the kinematic efficiency factor is 0.987, while for Xe and O is 0.450. Ne ions are efficient in transferring the kinetic energy to O anions than Xe ions. So, the light Ne ions are easy to change the O sub-lattice from order to disorder. Therefore, a lower transformation dose is required for Ne ion irradiation compared with Xe ion irradiation.

Previous ion irradiation experiments on fluorite structural derivative compounds indicate that the temperature–composition (T–C) phase diagram of compound is a good indicator that can predict the result of phase transformation induced by irradiation [22,27], which includes two main points: For the compounds which phases are stable to the melt, are readily amorphized by ion irradiation. However, for other compounds with ordered phase transform to disordered phase in T–C phase diagram, are resistant to ion irradiation. Furthermore, the ion irradiation amorphous dose depends on the O–D transformation temperature in the T–C phase diagram, the higher O–D transformation temperature, the higher ion irradiation amorphous dose [27]. From the T–C phase diagram of Lu_2O_3–HfO_2 [28] (not shown here), it is clear that the ordered δ-$Lu_4Hf_3O_{12}$ occurs thermal transformation to a disordered fluorite structure at about 1710 °C temperature before melting. For this reason, it is easy to understand the experimental result: $Lu_4Hf_3O_{12}$ undergoes a crystal structure transformation, from an ordered rhombohedral δ-phase structure, to a cubic disordered fluorite structure with increasing ion irradiation fluences.

5. Conclusions

In summary, we have concluded that δ-$Lu_4Hf_3O_{12}$ compounds undergo an order-to-disorder phase transformation under both light and heavy ion irradiation. Heavy ion irradiation induces an O–D transformation in δ-$Lu_4Hf_3O_{12}$ compounds, initiated at a fluence of 2×10^{13} ions/cm^2, and completed by a fluence of 1×10^{15} ions/cm^2 (~3.49 dpa). By contrast, this transformation dose is much higher than the O–D transformation dose induced by light Ne ion irradiation (~0.22 dpa). The large difference in O–D transformation threshold doses between Xe and Ne seems to suggest that heavy ions are less efficient than light ions in producing the retained defects during irradiation. The energy transfer kinetic factor also contributes to this difference. The order-to-disorder phase transformation of δ-$Lu_4Hf_3O_{12}$ compound is attributed to the effects of anion oxygen Frenkel-pairs defects. The T–C phase diagram is a good indicator of radiation-induced phase transformation in fluorite structural derivatives.

Acknowledgments

This work was sponsored by the National Natural Science Foundation of China (11175076, 10975065, 91026021 and 11135002).The work also sponsored by the U.S Department of Energy (DOE), Office of Basic Energy Sciences (OBES), Division of Materials Sciences and Engineering. The author wishes to thank the operators of the 320 kV platform for multi-discipline research with highly charged ions at the Institute of Modern Physics, CAS.

References

[1] K.E. Sickafus, R.W. Grimes, J.A. Valdez, A. Cleave, M. Tang, M. Ishimaru, S.M. Corish, C.R. Stanek, B.P. Uberuaga, Nat. Mater. 6 (2007) 217.
[2] R.C. Ewing, Proc. Natl. Acad. Sci. USA 96 (1999) 3432–3439.
[3] K.E. Sickafus, L. Minervini, R.W. Grimes, J.A. Valdez, M. Ishimaru, F. Li, K.J. McClellan, T. Hartmann, Science 289 (2000) 748.
[4] R.C. Ewing, W.J. Weber, J. Lian, J. Appl. Phys. 95 (2004) 5949.
[5] S.X. Wang, B.D. Begg, L.M. Wang, R.C. Ewing, W.J. Weber, K.V. Govidan Kutty, J. Mater. Res. 14 (1999) 4470–4473.
[6] R.C. Ewing, Pro. Nucl. Energy 49 (2007) 635–643.
[7] W.J. Weber, R.C. Ewing, C.R.A. Catlow, T. Diaz de La Rubia, L.W. Hobbs, C. Kinoshita, H.j. Matzke, A.T. Motta, M. Nastasi, E.K.H. Salje, E.R. Vance, S.J. Zinkle, J. Mater. Res. 13 (1998) 1434–1484.
[8] M. Ishimaru, Y. Hirotsu, M. Tang, J.A. Valdez, K.E. Sickafus, J. Appl. Phys. 102 (2007) 063532.
[9] K.E. Sickafus, M. Ishimaru, Y. Hirotsu, I.O. Usov, J.A. Valdez, P. Hosemann, A.L. Johnson, T.T. Thao, Nucl. Instr. Meth. B 266 (2008) 2892–2897.
[10] Y.H. Li, J. Wen, Y.Q. Wang, Z.G. Wang, M. Tang, J.A. Valdez, K.E. Sickafus, Nucl. Instr. Meth. B 287 (2012) 130–134.
[11] J. Lian, X.T. Zu, K.V.G. Kutty, J. Chen, L.M. Wang, R.C. Ewing, Phys. Rev. B 66 (2002) 71.
[12] J. Zhang, Y.Q. Wang, J.A. Valdez, M. Tang, K.E. Sickafus, J. Nucl. Mater. 419 (2011) 386–391.
[13] J.A. Valdez, M. Tang, K.E. Sickafus, Nucl. Instr. Meth. B 250 (2006) 148–154.
[14] J. Zhang, Y.Q. Wang, M. Tang, J.H. Won, J.A. Valdez, et al., J. Mater. Res. 25 (2010) 248.
[15] J.F. Ziegler, J.P. Biersack, U. Littmark. The stopping and range of ions in matter (SRIM). Available from: <http://www.srim.org>.
[16] Y.H. Li, B.P. Uberuaga, C. Jiang, S. Choudhury, J.A. Valdez, M.K. Patel, J. Won, Y.Q. Wang, M. Tang, D.J. Safarik, D.D. Byler, K.J. McClellan, I.O. Usov, T. Hartmann, G. Baldinozzi, K.E. Sickafus, Phys. Rev. Lett. 108 (2012) 195504.
[17] A. Guinier, X-Ray Diffraction in Crystals, Imperfect Crystals and Amorphous Bodies, Dover Publications, Inc., New York, 1994.
[18] G. Lim, W. Parrish, C. Ortiz, M. Bellotto, M. Hart, J. Mater. Res. 2 (1987) 471.
[19] D. Simeone, J.L. Bechade, D. Gosser, A. Chevarier, P. Daniel, H. Pilliaire, G. Baldinozzi, J. Nucl. Mater. 281 (2000) 171.
[20] K.E. Sickfaus, R.W. Grimes, S.M. Corish, A.R. Cleave, M. Tang, C.R. Stanek, B.P. Uberuaga, J.A. Valdez, Layered Atom Arrangements in Complex Materials, Los Alamos Series, Report # LA-14205, 2006.
[21] Z.L. Zhang, H.Y. Xiao, X.T. Zu, F. Gao, W.J. Weber, J. Mater. Res. 24 (2009) 1335.
[22] Y.H. Li, Y.Q. Wang, M. Zhou, C.P. Xu, J.A. Valdez, K.E. Sickafus, Nucl. Instr. Meth. B 269 (2011) 2001.
[23] L.J. Chen, et al., submitted to publication.
[24] S.J. Zinkle, Microstructure of ion-irradiated ceramic insulators, Nucl. Instr. Meth. Phys. Res. Sect. B 91 (1994) 234.
[25] S.J. Zinkle, Effect of irradiation spectrum on the microstructural evolution in ceramic insulators, J. Nucl. Mater. 219 (1995) 113.
[26] S.J. Zinkle: Irradiation spectrum and ionization-induced diffusion effects in ceramics, in Microstructure Evolution During Irradiation, in: I.M. Robertson, G.S. Was, L.W. Hobbs, T. Diaz de la Rubia (Eds.), Proc. Mater. Res. Soc. Symp., vol. 439, Warrendale, PA, 1997, p. 667.
[27] J. Zhang, Y.Q. Wang, M. Tang, J.A. Valdez, K.E. Sickafus, Nucl. Instr. Meth. B 268 (2010) 3018.